The microRNA-processing enzyme DICER is dispensable for somite segmentation but essential for limb bud positioning

Zhen Zhang[1], **Jason R. O'Rourke**[2], **Michael T. McManus**[3], **Mark Lewandoski**[4], **Brian D. Harfe**[2], and **Xin Sun**[1]

[1]Laboratory of Genetics, University of Wisconsin-Madison, Madison, WI 53706

[2]Department of Molecular Genetics and Microbiology, University of Florida College of Medicine, Gainesville, FL 32610

[3]Department of Microbiology and Immunology Diabetes Center, University of California, San Francisco, CA 94143

[4]Cancer and Developmental Biology Lab, National Cancer Institute, Frederick, MD 21702

Abstract

DICER is an enzyme that processes microRNAs (miRNAs) to their mature forms. As miRNAs were first discovered for their role in the control of developmental timing, we investigated their potential requirement in mouse somitogenesis, an event with precise temporal periodicity. To address the collective role of miRNAs in mesoderm development including somite formation, we used *T*(*Brachyury*)-Cre mouse line to inactivate *Dicer* in most cells of the mesoderm lineage. This *Dicer* mutant exhibits a reduced anterior-posterior axis. Somite number remains normal in mutant embryos up until the death of the embryos more than two days after *Dicer* inactivation. Consistent with this, the molecular machineries required for establishing segmentation, including clock and wave front, are not perturbed. However, somite size is reduced and later-formed somites are caudalized, coincident with increased cell death. Outside of the paraxial mesoderm and prior to apparent reduction of the axis in the mutant, the position of the hindlimb bud, a lateral plate mesoderm-derived structure, is posteriorly shifted and the timing of hindlimb bud initiation is delayed accordingly. We observed changes in the expression of genes critical for limb positioning, which include a shifted and delayed downregulation of *Hand2* and *Tbx3*, and shifted and delayed upregulation of *Gli3* in the prospective limb bud field. The 3′UTRs of both *Hand2* and *Tbx3* harbor target sites for a seed sequence-sharing cluster of miRNAs *mir-25/32/92/363/*367. As an example of the cluster, we show that *mir-363*, a miRNA with elevated expression in the prospective limb bud field, is capable of inhibiting *Hand2/Tbx3* expression in vitro in a binding site-dependent manner. Together, our findings provide the first demonstration that in mouse embryonic mesoderm, while *Dicer* is dispensable for somite segmentation, it is essential for proper limb bud positioning.

Keywords

limb; limb positioning; somite; *Dicer*; microRNA; mouse

Author for correspondence: Xin Sun, Phone: (608)265-5405, Fax: (608)262-2976, xsun@wisc.edu.

Introduction

DICER is an RNase III enzyme that processes microRNAs (miRNAs) and small interfering RNAs (siRNAs) to their mature ~22 nucleotide (nt) forms. In animals, the majority of mature miRNAs functions by forming imperfect base pairs with the 3′UTR region of their target gene mRNAs and triggering translation repression (for review, see Bartel, 2009). It was recently shown that these miRNAs can also elicit a reduction in target transcript level, especially for the most highly repressed targets (Baek et al., 2008; Selbach et al., 2008). To date, 590 mouse miRNAs and 940 human miRNAs have been registered in the miRBase (http://www.mirbase.org/cgi-bin/browse.pl). It is estimated that ~30% of genes in either of these mammalian genomes may be regulated by miRNAs (Lewis et al., 2005).

The first miRNA identified, *lin-4*, is a factor that regulates the timing of larval development in *C. elegans* (Lee et al., 1993). Since then, miRNAs have been found to function in a wide spectrum of biological processes during embryogenesis (for review, see Stefani and Slack, 2008). Multiple miRNAs are expressed in spatially restricted patterns in vertebrate embryos (Darnell et al., 2006; Wienholds et al., 2005). Little is known about their requirements in the patterning of early embryos. In this study, we investigate the collective role of miRNAs in the early mesoderm, focusing on somite formation and limb bud initiation.

Somites are pairs of mesodermal blocks of cells that line each side of the neural tube along the anterior-posterior (A-P) axis of vertebrate embryos. They give rise to adult skeletal muscles, axial skeleton and dorsal dermis. Somites are generated from presomitic mesoderm (PSM) cells at regular time intervals as a result of segmental patterning. Several signaling pathways including NOTCH, WNT and FGF play important roles in this process (for review, see Dequeant and Pourquie, 2008). In mouse, the expression of NOTCH pathway components such as *Lunatic Fringe* (*Lfng*) oscillates in the posterior PSM. The oscillating waves sweep through the PSM in a posterior to anterior direction. The regular intervals of this oscillation ensure the periodicity of segmentation. When each wave reaches the anterior PSM at a molecular boundary termed the wave front, the oscillation is suspended and a pair of somites will epithelialize and form segment boundary. The precise position of this wave front is determined dynamically by a balance between the posterior-to-anterior FGF signaling gradients, and the anterior-to-posterior retinoic acid (RA) gradient (Diez del Corral et al., 2003; L. A. Naiche, 2010; Moreno and Kintner, 2004). In the anterior PSM, the rostral-caudal (R-C) polarity of future somites is determined just prior to segment boundary formation. Both R-C patterning and segment boundary formation are dependent on the activity of shorter range signaling pathways such as the NOTCH pathway (Saga, 2007).

Vertebrate limbs initiate as limb buds at stereotypical positions along the body axis. Several mouse mutants, including null mutations in Hox8, Hox9 paralogous group genes and *Gdf11* show shifts in limb bud position (McIntyre et al., 2007; McPherron et al., 1999; van den Akker et al., 2001). In addition, a study in chick shows that altering the spatial relationships of transcription factors expressed in the LPM, including *Tbx3*, *Hand2* and *Gli3* leads to limb bud position shifts (Rallis et al., 2005). While these studies reveal players in the genetic program that control limb bud position, their upstream regulators, downstream mediators, and their relationship with each other remain unknown.

As somite and limb bud positioning are regulated by multiple molecular pathways in a dynamic fashion, it is critical that the spatial and temporal expression of these molecules be precisely regulated. To address if miRNAs play a role in regulating gene expression in these developmental processes, we inactivated *Dicer* in the mesodermal lineage in mouse. There is only one *Dicer* gene in the mouse genome, and it encodes the principal enzyme that processes miRNAs and endogenous siRNAs. Inactivation of *Dicer* has proven an effective

approach to discern the collective role of miRNAs and endogenous siRNAs in various developmental settings. For example, analysis of *Dicer* null mutants shows that *Dicer* is essential for stem cell maintenance in the early gastrula (Bernstein et al., 2003). Analysis of mutants with skeletal muscle specific knockout of *Dicer* shows that it is required to maintain muscle cell survival (O'Rourke et al., 2007). A study from our laboratory on mutants with lung epithelium-specific knockout of *Dicer* shows that it is essential for lung branching morphogenesis (Harris et al., 2006).

In this study, we conditionally inactivated *Dicer* in mesoderm cells shortly after their emergence from the primitive streak. In mutant embryos, somites appear to form on schedule, despite increased cell death. Those somites that epithelialize after Embryonic Day (E)10 are caudalized, likely a result of excess cell death at the anterior PSM. In addition to these defects in paraxial mesoderm, we found that the position of the hindlimb bud is shifted three somites posteriorly which is correlated with a delayed downregulation of *Hand2* and *Tbx3* in the posterior limb bud field and a delayed activation of *Gli3* in the anterior limb bud field. In light of the evidence, we conclude that in the paraxial mesoderm, *Dicer* is essential to maintain cell survival, but is dispensable for PSM segment boundary formation. In the lateral plate mesoderm (LPM), *Dicer* controls limb bud position, possibly in part by downregulating *Hand2* and *Tbx3* in the prospective limb field.

Results

Inactivation of *Dicer* in mesoderm leads to reduction of A-P axis length

To bypass the early requirement for *Dicer* during gastrulation and investigate its role in somite development, we inactivated *Dicer* using a conditional allele (*Dicer^flox^*) and a *Tcre* transgenic strain in which the Cre recombinase is driven by the *T* (*Brachyury*) promoter (Harfe et al., 2005; Perantoni et al., 2005). We generated embryos that are either *Tcre;Dicer^del/flox^* or *Tcre;Dicer^flox/flox^* and they are phenotypically indistinguishable from one another (hereafter collectively referred to as *Tcre;Dicer* or mutant), while *Tcre;Dicer^flox/+^* and *Tcre;Dicer^del/+^* embryos are normal and therefore are used as controls. In *Tcre;Dicer* mutant embryos, we assessed *Dicer* inactivation by RNA whole mount in situ hybridization using a probe that hybridizes to sequences deleted following cre-mediated recombination in the *Dicer* conditional allele. In control embryos, *Dicer* mRNA is detected ubiquitously along the entire A-P axis at E8.5 and 9.0 (Supplemental Fig. 1A-C). In the mutant at E8.5, active *Dicer* transcripts are still detected in mesoderm and neuroectoderm (Supplemental Fig. 1A). By E9.0 in mutant embryos, *Dicer* transcripts are no longer detected in most mesodermal tissues posterior to the heart, consistent with where *Tcre* is active (Supplemental Fig. 1B,C) (Perantoni et al., 2005). To confirm that maturation of miRNAs is blocked in the mutant embryos, we performed Northern blot analysis to detect miRNAs *mir-1*, *mir-133*, *mir-10b* and *mir-196a*, using RNA from the posterior portion of E10.5 embryos starting from the hindlimb-bud level. These miRNAs were chosen because they have been shown to be expressed in the myotome, posterior trunk and/or tailbud (Kloosterman et al., 2006). We found that mutant embryos display a severe reduction of all these miRNAs in their mature forms (Supplemental Fig. 1D). The residual amount of *mir-10b* is likely processed in posterior surface ectoderm and neural tube where Cre expression is not complete (Perantoni et al., 2005). Consistent with the decrease in mature forms, the precursor forms of these miRNAs are detected at a higher level in the mutant (Supplemental Fig. 1D and data not shown). These results suggest that following *Dicer* inactivation in the mesoderm, miRNAs are no longer processed into their mature forms in this tissue.

The morphological defects in *Tcre;Dicer* embryos are first detected at ~E10.5. Compared to control littermates, the mutant embryos exhibit reduced A-P axis length, especially in the

posterior half of the axis where *Dicer* inactivation is more complete (Fig. 1A–D). This reduction is quantified by measuring the length of A-P axis from posterior boundary of forelimb buds to tail tip between mutant and controls at three stages (Fig. 1G). The mutant embryos at 35-somite and 52-somite stages exhibit significantly reduced A-P length ($p<0.05$, $n>4$ for each stage), in contrast to mutants at 28-somite stage which show normal length. Mutant embryos start to die at approximately E12.5, possibly due to hemorrhaging (data not shown), and are not recovered past E13.5. This is consistent with a recent study showing that *Dicer* is essential for angiogenesis in mouse embryos (Yang et al., 2005).

Inactivation of *Dicer* leads to increased cell death and reduced somite size, but not number

The shortening of A-P axis length in *Tcre;Dicer* embryos could be due to either reduced somite number or somite size. We found that mutant embryos contain a comparable number of somites as control littermates at E10.5 (37–38 somites, Fig. 1A,B), and at E11.5 (51 somites, Fig. 1C,D) when the A-P reduction is apparent. However, the somites in mutant embryos are smaller than in controls (Fig. 1E,F). These results suggest that a reduction in somite size, but not somite number, contributes to axis shortening.

Several possibilities may contribute to the reduction of somite size in the mutant: each somite could contain the same number of cells that are either smaller in size or more densely packed into a smaller space, or each somite could consist of fewer cells. From the sagittal sections of the tail region of E11.5 mutant embryos (Supplemental Fig. 2), we found that cells in the somites are not smaller or more densely packed. Instead, we found that there are fewer cells in each somite, likely contributing to the reduction of somite size.

Fewer cells in mutant somites could be due to a defect in cell proliferation or an increase in cell death. By labeling proliferating cells with an antibody specific to phosphorylated-Histone H3 (PH3), we detected no significant difference in the proportion of PH3 positive cells in the somites of E10.5 mutants compared to control (data not shown). To test if there is increased cell death in the mutant somites, we carried out LysoTracker staining in embryos from E8.75 to E11.5. We detected a progressive increase in cell death in the mutant embryos. At E8.75 (14–16 somites), increased cell death is only detected in the 5th and 6th somites (n=3/3, Fig. 1H,I). At later stages, the posterior boundary of increased cell death extends, while the anterior boundary remains the same (Fig. 1J–O). This posterior boundary is anterior to the most nascent 2–3 somites at approximately E9.5 (n=6/6, Fig. 1J), extends into the anterior PSM region at E10.0 (n=4/4, Fig. 1M), and encompasses the entire PSM region by E11.0 (n=3/3, Fig. 1O and data not shown). Compared to the paraxial mesoderm, there is only a slight increase in cell death in the mutant LPM versus control (Fig. 1P,Q).

We next addressed whether increased cell death within each mutant somite is specific to one of the three cell compartments representing dermomyotome, myotome and sclerotome. We performed TUNEL analysis and cleaved CASPASE 3 immunostaining in transverse sections of E10.5 embryos at the forelimb bud level (somite 7–12) where the three cell compartments are delineated. Control embryos display a low level of cell death (Supplemental Fig. 3D). Mutant embryos, however, show an increased level of cell death in the dermomyotome and sclerotome, but not in the myotome as identified by MYF5 expression (Supplemental Fig. 3A–C). This differential increase in cell death is transient because by E11.5, cell death is observed in all three somite compartments (Supplemental Fig. 3E–G). Interestingly, this dynamic pattern of cell death correlates with the changing cell proliferation patterns indicated by BrdU labeling and PAX3/PAX7-positive proliferating cells (Gros et al., 2005; Relaix et al., 2005). At a stage before the epithelial-mesenchymal transition (EMT) of dermomyotome, cell proliferation is high in dermomyotome and sclerotome but low in the myotome. After dermomyotome EMT, cell proliferation is high across all three

compartments. To directly examine the relationship between myotome cell proliferation and cell death in the *Dicer* mutant, we followed proliferating cells in the somites by their expression of PAX7 (Relaix et al., 2005). In E10.5 mutants, the myotome region is negative for both PAX7 and cell death (Supplemental Fig. 3I–K). However at E11.5, PAX7 is now expressed in the myotome, and some of these PAX7-positive cells undergo apoptosis (Supplemental Fig. 3M–O). Together, these data suggest that in *Tcre;Dicer* somites, increase of cell death occurs in regions where cells normally undergo proliferation. This is consistent with previous observation that inactivation of *Dicer* in cultured cells leads to premature sister chromatid separation during cell proliferation, and subsequent cell death (Fukagawa et al., 2004).

Inactivation of *Dicer* does not perturb paraxial mesoderm segmentation

The observation that somite number remains normal in *Tcre;Dicer* embryos at E11.5 suggests that somites continue to form in the absence of *Dicer*. We further examined the rate of somite formation by harvesting embryos at regular intervals between E9 and E11.5 to compare somite number in mutant versus control embryos. We did not detect any delay in new somite addition and somite boundaries form normally in mutant embryos compared to control littermates (Fig. 1, Fig. 3A–F,A′-F′ and Supplemental Fig. 2). This suggests that the molecular machinery that is required for PSM segmentation still operates in mutant embryos until at least E11.5, approximately 2.5 days after *Dicer* inactivation (Supplemental Fig. 1B,C). To confirm this, we examined the *Fgf8* gradient and *Lfng* oscillation, two parameters involved in segmentation. We detected *Fgf8* mRNA in a normal pattern in the PSM region of mutant embryos at E10.5 (n=2 Fig. 2A and B). In addition, we found that *Spry2*, a transcriptional readout of FGF activity, is expressed in a normal pattern in the PSM of mutant embryos (Fig. 5I,L). At E10.5, we identified all three phases of *Lfng* oscillation patterns in the PSM of mutant embryos (Fig. 2C–H), although *Lfng* expression is reduced in intensity, possibly due to increased cell death. These data suggest that the molecular machinery responsible for PSM segmentation remains intact following *Dicer* inactivation.

Inactivation of *Dicer* leads to caudalization of somites after increased cell death is detected in the anterior PSM

To address the requirement for *Dicer* in somite R-C patterning, we assayed for the expression of caudal markers, *Uncx4.1* and *Dll1*, and the rostral marker *Tbx18*. In the mutant embryos, all somites formed prior to E10 show normal R-C polarity (Fig. 3A–B′,I,J). At E10 and thereafter, the newly formed somites are caudalized, as shown by the expansion of rostral markers *Uncx4.1* and *Dll1* expression into the entire somite, and loss of caudal marker *Tbx18* expression (Fig. 3C–L). Previous studies show that *Mesp2* expressed in the anterior PSM is essential for establishing the R-C polarity of nascent somites. When it is reduced, the somites that subsequently form are caudalized (Saga et al., 1997; Nomura-Kitabayashi et al., 2002). We found that at E9.5 when somite polarity is normal, the expression of *Mesp2* in *Tcre;Dicer* mutant embryos is comparable to control (Fig. 3M and N). However, starting at E10, we observed a significant decrease in *Mesp2* level in the mutant embryos compared to control (n=5/5), coinciding with caudalization of nascent somites in the mutant (Fig. 3O–R). The expression of *Mesp2* downstream genes, *Cer1*, *Eph4A* and *PAPC*, is normal at E9.5 but is reduced at E10.5 in mutant embryos compared to control (n=2/2 each, Fig. 3S–V and data not shown). In addition, the expression of *Ripply2*, a negative regulator of *Mesp2* expression, is also reduced in the mutants at E10.5 (n=2/2, Fig. 3W and X) (Morimoto et al., 2007). These data suggest that a reduction in *Mesp2* expression is consistent with caudalization of the somites in *Tcre;Dicer* embryos. We note that starting at E10.0, increased cell death is observed in anterior PSM cells where *Mesp2* is expressed (Fig. 1L,M). This correlation raises the possibility that downregulation of *Mesp2* and caudalization of somites observed after E10 may be secondary to increased cell death.

Inactivation of *Dicer* leads to a posterior shift and delayed formation of hindlimb buds

Outside of the paraxial mesoderm, we found that the position of the hindlimb bud, a LPM-derived structure, is shifted posteriorly for three somites, from position somite 25–29 to somite 28–32 (Fig. 4A,B). This hindlimb phenotype is observed with consistent expressivity and full penetrance, while the forelimb forms in a normal position. At the ~28-somite stage just prior to when hindlimb bud initiate, although there is no significant difference in the length of both AP axis and LPM between mutant and control embryos (Fig. 1G and 4E), the expression domains of some genes involved in limb initiation are already altered in the mutants. For example, the expression of *Tbx4*, one of the earliest hindlimb bud markers, is shifted posteriorly before limb bud outgrowth (Fig. 4C,D). Furthermore, signals essential for limb bud initiation and outgrowth, such as FGF and WNT, are activated later and in a more posterior position in the mutant compared to control as indicated by the expression of either ligand (*Fgf8, Fgf10*) or activity readouts (*Spry2* for FGF, and *Axin2* for WNT) (Fig. 5). A previous study shows that *Spry2* is upregualted in late-stage limb bud from a different *Dicer* mutant where *Dicer* is inactivated at a later time than ours (Harfe et al., 2005). In the *Tcre;Dicer* limb buds, however, there is no apparent increase in *Spry2* expression at ~E10.25 compared to control, possibly due to timing differences between the two mutants. In *Tcre;Dicer* embryos, consistent with the molecular changes, hindlimb bud initiation is delayed by approximately six hours compared to control, corresponding with the emergence of LPM cells adjacent to the three additional somites. Subsequent development of the hindlimb bud continues to be delayed. For example, the temporal changes of the expression domains of *Hoxa11* and *Hoxa13*, the zeugopod and autopod markers of limb buds, occur later in the mutant hindlimb compared to control (Supplemental Fig. 4). The shift of gene expression domains before A-P axis shortening and the overall delay of hindlimb development suggest that the hindlimb bud defects in the mutant cannot solely be attributed to axial tissue shortening, and *Dicer* may play a direct role in limb positioning.

Posterior shift of hindlimb bud is accompanied by altered transcription of *Hand2, Tbx3, Gli3*, but not *Gdf11* and Hox genes

Previous studies show that inactivation of Hox8 or Hox9 paralogous groups of genes leads to posterior shift of hindlimb position (McIntyre et al., 2007; van den Akker et al., 2001). Furthermore, it has been shown that the expression of Hox9 paralogous group genes shifts with change in limb bud identity (Cohn et al., 1997). To address if these Hox genes may mediate *Dicer* function in the mesoderm, we assayed for their expression by RNA in situ hybridization. In *Tcre;Dicer* mutants at E10.25, all Hox genes examined, including *Hoxb8, c8, b9,c9* and *d9* appear to be expressed in their normal domain in both the axial mesoderm and LPM (n 3 each, Fig. 6A–D and data not shown). Hindlimb bud shift has also been observed in the *Gdf11* mutant. In the *Gdf11* mutant, it was shown that the expression domains of several Hox genes, including *Hoxc8*, *Hoxc10* and *Hoxc11*, are shifted, suggesting that *Gdf11* may act through Hox genes (McPherron et al., 1999). We examined the expression of *Gdf11* and its downstream Hox genes in the *Dicer* mutant by RNA in situ hybridization. We found that their expression domain and intensity are not altered (n 2 each, Fig. 6E–H and data not shown). Normal expression of these genes argues against the possibility that *Dicer* controls limb positioning via regulating *Gdf11* or Hox transcription. However, it remains possible that *Dicer* may act in this process by regulating them at the protein level.

A recent study shows that the balance among three transcription factors, TBX3, HAND2 and GLI3 in the LPM-derived prospective limb field is critical for limb positioning (Rallis et al., 2005). Overexpression of *Tbx3*, or interference of normal *Gli3* repressor function prior to limb bud initiation leads to an expansion of *Hand2* expression domain, and a shift of limb bud position. To investigate if an alteration in the balance of *Hand2/Tbx3/Gli3* antagonism

may be responsible for the limb bud shift in the *Tcre;Dicer* mutant, we examined their expression during hindlimb bud establishment. In control embryos just prior to hindlimb bud initiation (somite 28 stage), we observed a downregulation of *Hand2* (n=4/4) and *Tbx3* (n=5/5), and a concomitant upregulation of *Gli3* (n=3/3) in the anterior region of the prospective limb bud field (Fig. 7A,C,E). In mutant embryos at the same stage however, *Hand2* (n=4/4) and *Tbx3* (n=3/3) remains expressed throughout the limb bud field while *Gli3* (n=2/2) expression remains relatively low (Fig. 7B,D,F). Quantitative RT-PCR further confirmed the downregulation of *Hand2* and *Tbx3* and upregulation of *Gli3* in the control but not mutant embryos at ~28 somite stage (Fig. 7G–I). Downregulation of *Hand2* eventually occurs in mutants at 31 somite stage, in a more posterior position where the hindlimb buds finally initiates in mutant embryos (Fig. 7J–O). These results suggest that there is a delay and posterior shift of *Hand2*, *Tbx3* downregulation and *Gli3* upregulation in the *Tcre;Dicer* mutant prospective hindlimb field.

Hand2 and Tbx3 3′UTRs contain target sites for *mir-363*

To explore if miRNAs play a roles in regulating the balance of *Hand2/Tbx3/Gli3* expression in the prospective hindlimb bud region, we searched the 3′ untranslated region (UTR) of *Hand2* and *Tbx3* for target sites of miRNAs using TargetScan and PicTar, two frequently used miRNA target prediction programs (Baek et al., 2008; Krek et al., 2005; Lewis et al., 2003). In *Hand2* 3′UTR there are two sites predicted by both programs. One is a confirmed target site of *mir-1* (Zhao et al., 2005), and the other is targeted by *mir-25/32/92/363/367*, a family of miRNAs that share the same seed sequence (Fig. 8A). In *Tbx3* 3′UTR, the sites predicted by both programs are targeted by *mir-137*, *mir-153* and interestingly, *mir-25/32/92/363/*367. Each of the *mir-25/32/92/363/367* target sites in *Hand2* and *Tbx3* 3′UTR is evolutionarily conserved across multiple vertebrate species from chick to human (data not shown). To address if any of these miRNA may impact *Hand2/Tbx3* expression, we chose *mir-363* as an example for further study since it is reported to be expressed at a higher level in the prospective limb bud field compared to the interlimb LPM in chick (Darnell et al., 2006). To confirm that *mir-363* is expressed in the limb bud field in mouse, we performed quantitative RT-PCR to analyze the level of mature *mir-363* in forelimb region at ~23-somite stage when forelimb bud initiates, and in hindlimb and interlimb regions at ~28-somites stage when the hindlimb bud initiates (Fig. 8B). We found that in control embryos *mir-363* is indeed expressed in forelimb and hindlimb bud fields, and its expression level in hindlimb field is approximately two fold as high as in interlimb region (p<0.05, n=3). Furthermore, in the *Dicer* mutant in the forelimb region during bud initiation, although mature *mir-363* level is reduced compared to control, it remains present. However, in the hindlimb region during bud initiation, mature *mir-363* level is almost undetectable. Loss of *mir-363* in the mutants offers an example for the extent of overall miRNA inactivation and clearance. We postulate that the persistence of residual miRNAs in the forelimb bud region may support bud initiation at its normal position, while severe abrogation of miRNAs in the prospective hindlimb bud region leads to shift of bud.

To test if *mir-363* is capable of regulating *Hand2* and *Tbx3* expression through binding to the predicted sites, we inserted the *Hand2* or *Tbx3* 3′UTR sequence downstream of luciferase and measured the level of luciferase activity in the presence or absence of *mir-363* transfection in Hela cells. We found that addition of *mir-363* led to a statistically significant downregulation of luciferase activity with either *Hand2* or *Tbx3* 3′UTR (Fig. 8C). Furthermore, this downregulation is abolished by mutating the sequence of the predicted site in either of the 3′UTR. These data suggest that *mir-363* inhibits *Hand2* and *Tbx3* expression in vitro, and this inhibition is dependent on intact target sites in their 3′UTR region.

Discussion

In this study, we inactivated *Dicer* in mesodermal cells using Cre-mediated recombination. This leads to increased cell death and a shortened A-P axis. However, segmentation of paraxial mesoderm occurs on schedule, suggesting that collectively, miRNAs are not required for this reiterative developmental event. *Tcre;Dicer* mutants exhibit posterior shift of hindlimb bud with complete penetrance, providing strong evidence that *Dicer* is essential for controlling hindlimb bud position. Our data raise the possibility that miRNAs control the balanced expression of *Hand2/Tbx3/Gli3* in the prospective limb bud field, and in turn contribute to proper positioning of limb buds.

Dicer is dispensable for PSM segmentation

Several lines of evidence prompted us to examine the requirement for *Dicer* and miRNAs in somite formation. miRNAs were first identified as regulators of developmental timing in *C. elegans* (Lee et al., 1993; Wightman et al., 1993). In vertebrate development, somitogenesis is arguably one of the best-studied processes involving dynamic control of developmental timing. Furthermore, in vertebrate somite formation, strong evidence suggests that members of the Notch pathway, in particular *Hes1* and *Hes7*, play critical roles (Bessho et al., 2001; Jouve et al., 2000; Palmeirim et al., 1997). These genes are homologs of *Drosophila Enhancer of Split* (*E(spl)*), which have been shown to be regulated by miRNAs (Lai et al., 2005). Thus it is interesting that more than two days after inactivation of *Dicer* transcript in the *Tcre;Dicer* mutant (from E9.0 to E11.5) and with a clear loss of mature miRNAs, somites continue to generate at a normal rate. In addition, *Fgf8* and *Lfng* expression patterns indicate that the wave front and the NOTCH oscillator, respectively, remain normal in this mutant. Thus our data from *Tcre;Dicer* mutants suggest that miRNAs are not required for maintaining the clock/wave front mechanism in mouse. This finding is consistent with data from zebrafish showing that embryos lacking maternal and zygotic *Dicer* form normally spaced somites at early stages of development (Giraldez et al., 2005). Current evidence suggests that the dynamic molecular program that drives somitogenesis is achieved mainly via a series of feedback regulations at the transcriptional level (Dequeant and Pourquie, 2008).

Dicer is essential for paraxial and lateral plate mesoderm cell survival

The increased cell death observed in *Tcre;Dicer* embryos occurs in progressively larger cell populations as development proceeds. Along the A-P axis, increased cell death is first observed in somite 5 and 6 at E8.75, before its posterior spread. It is unclear why increased cell death is not detected in the anterior-most four somites. It is known that unlike the posterior somites that undergo resegmentation to form vertebrae, these four somites fuse to form the basioccipital skeletal elements of the skull (Huang et al., 2000). Thus it is conceivable that they are under the control of a different molecular program compared to the more posterior somites, and this difference may render them independent of *Dicer* for survival. Alternatively, as these four somites form at the anterior extremity of *Dicer* inactivation domain by Tcre (Supplemental Fig. 1B), it is possible that *Dicer* inactivation may not be as complete in these somites as compared to the more posterior ones in the mutant embryo.

Within a somite, the correlation of cell death and cell proliferation in the myotome suggests that proliferating cells are more sensitive to loss of *Dicer*. In cell culture, it was shown that inactivation of *Dicer* leads to disruption of heterochromatin, and in turn premature sister chromatid separation during cell proliferation (Fukagawa et al., 2004). This eventually results in death of proliferating cells in culture. This role in the maintenance of

heterochromatin may explain the correlation between cell proliferation and cell death in the *Tcre;Dicer* mutant in vivo.

Within a somite on the R-C axis, even though cell death is evenly distributed across the somite, progressive expansion of the cell death domain into the PSM may also explain the caudalization of nascent somites in the *Dicer* mutant. Previous studies show that *Mesp2* expressed in the anterior PSM triggers cell-non-autonomous feedback regulation that is essential for R-C polarity. In *Mesp2* hypomorphic mutants, somites are caudalized while somite boundaries are relatively normal (Nomura-Kitabayashi et al., 2002). The similarity between *Mesp2* hypomorphic and *Tcre;Dicer* mutants suggests that the reduction of *Mesp2* observed in *Tcre;Dicer* PSM may contribute to the loss of polarity phenotype. It is possible that miRNAs positively regulate the expression of *Mesp2* indirectly through repressing intermediate miRNA target(s). However, in light of the evidence that increased cell death is first detected in the *Mesp2*-expressing anterior PSM at the same time when somites lose their polarity, it is more likely that this cell death led to the apparent downregulation of *Mesp2* and subsequent caudalization of somites.

DICER is essential for hindlimb positioning

The *Tcre;Dicer* mutant exhibits posterior shift of hindlimb with full penetrance. Since the limb bud position is measured against somites, an important possibility to consider is that the limb bud shift may be entirely attributed to relative shrinking of the paraxial mesoderm past the prospective hindlimb LPM. However, several observations argue against this possibility. First, the hindlimb bud initiation program, as measured by *Tbx4* expression and FGF and WNT signaling, is altered prior to the stage when paraxial shortening becomes obvious. Second, the development of hindlimb is delayed for about six hours in mutant, a temporal phenotype not easily explained by the spatial shortening of the axis. Third, the hindlimb shift is also evident with a comparison to markers within the LPM. For example, all Hox genes assayed show normal spatially restricted expression not only in the paraxial mesoderm, but also in the LPM (e.g. Fig. 6G,H). Compared to Hox LPM boundaries, the hindlimb bud is shifted. Together, these lines of evidence suggest that the requirement for *Dicer* in limb bud positioning is independent of its role in maintaining paraxial mesoderm length.

In a wild-type embryo, it remains unclear whether limb bud initiation is triggered by upstream molecular events in the LPM, intermediate mesoderm or somites. Recent studies argue against the possibility that signals from the intermediate mesoderm are required for limb bud initiation (Boulet et al., 2004; Fernandez-Teran et al., 1997; Perantoni et al., 2005). Classical experiments suggest that signals from the somite may be important for limb bud initiation (Gibert et al., 2006; Martin, 1998). However, the nature of this somite-derived signal(s) has not been elucidated. Recent studies show that transcription factors expressed in the LPM, *Tbx4* and *Tbx5*, are essential for proper limb bud initiation (Agarwal et al., 2003; Minguillon et al., 2005; Naiche and Papaioannou, 2003), raising the possibility that the upstream events for limb bud initiation may take place within the LPM.

Misregulation of *Hand2/Tbx/Gli3* expression by miRNAs may contribute to hindlimb position shift

To probe the molecular changes underlying the limb bud shift phenotype observed in *Tcre;Dicer* mutant, we started with genes that have been implicated in limb bud positioning. Previous studies show that limb bud shifts are often associated with changes in axial skeleton and Hox expression. While *Tcre;Dicer* embryos die too early to allow analysis of the axial skeletal identity, we are able to discern axial patterning via examining gene expression. We found that the expression of *Gdf11*, as well as its downstream effector genes

Hoxc10 and *Hoxc11* remains normal, suggesting that *Dicer* does not act via *Gdf11* for limb bud positioning. Furthermore, we detected no shift in the expression of additional Hox genes, suggesting that *Dicer* function in this process may not be mediated through Hox genes.

In contrast to the lack of a change in *Gdf11* and Hox expression, we detected a spatial and temporal alteration in *Hand2/Tbx3/Gli3* expression in accordance with the limb bud shift in *Tcre;Dicer* mutants. Although none of these genes are essential for limb bud initiation, a recent study provides strong evidence supporting a model that interactions among *Hand2*, *Tbx3* and *Gli3* in the limb bud forming region plays an important role in determining limb bud position (Rallis et al., 2005). This raises the possibility that the observed changes in *Hand2/Tbx3/Gli3* balance may contribute to limb bud shift in the *Tcre;Dicer* mutant.

To explore the cause for the altered *Hand2/Tbx3/Gli3* expression, we identified binding sites for a number of miRNAs in the 3′UTRs of *Hand2* and *Tbx3*. As an example among them, we show that *mir-363*, a miRNA with elevated expression in the prospective limb bud region, can downregulate *Hand2* and *Tbx3* expression in vitro. In vivo, we speculate that it is likely that a combination of miRNAs function together to impact *Hand2/Tbx3* expression and limb bud positioning. Based on our findings, we propose the following model (Fig. 8D). In a normal embryo, miRNAs such as *mir-363* target *Hand2* and *Tbx3* 3′UTRs and downregulate their expression at the protein level in the anterior half of prospective limb bud field. This in turn allows the upregulation of *Gli3*. Based on previous data (Rallis et al., 2005; te Welscher et al., 2002), GLI3 is capable of inhibiting *Hand2* and *Tbx3* at the transcript level, thus reinforcing the downregulation of *Hand2* and *Tbx3* RNA. Local reduction of HAND2 and TBX3 positions the limb bud for initiation. In the *Tcre;Dicer* mutant in the normal prospective hindlimb bud region (somite 25–29), due to absence of mature miRNAs, HAND2 and TBX3 expression is no longer attenuated at the protein level. *Gli3* fails to upregulate, which allows the observed persistence of *Hand2* and *Tbx3* transcripts. Failure of HAND2/TBX3 downregulation precludes limb bud initiation in the normal hindlimb bud region. For this model to accurately explain the *Tcre;Dicer* phenotype, it also requires that in the absence of miRNA, there is a backup mechanism in place to downregulate *Hand2/Tbx3* in a more posterior position than normal. While this mechanism is hypothetical, the same mechanism may be at play in other existing mutants that show posterior shift of hindlimb buds (McPherron et al., 1999).

In support of this model (Fig. 8D), overexpression of *Tbx3* in chick leads to reduced *Gli3*, failed downregulation of *Hand2* and shift of limb bud (Rallis et al., 2005). It is interesting to note that despite similarities on the molecular level, *Tbx3* overexpression leads to an anterior shift of limb bud while inactivation of *Dicer* leads to a posterior shift of limb bud. This phenotypic difference may be traced back to their distinct effects on the domain of *Hand2/Tbx3* expression. Overexpression of *Tbx3* in chick LPM results in an anterior shift of the low HAND2/TBX3 versus high HAND2/TBX3 boundary, leading to the establishment of limb bud in a more anterior location at approximately the same time as normal limb bud initiation. In contrast, in the *Tcre;Dicer* mutant, HAND2/TBX3 are not downregulated at the normal timeframe of hindlimb bud initiation. They are only downregulated at a later time, creating the low HAND2/TBX3 versus high HAND2/TBX3 boundary in a more posterior location, leading to the delay and posterior shift of limb bud. It is important to emphasize that since inactivation of *Dicer* leads to disruption of all mature miRNAs, the limb bud shift is likely a result of combined effects of loss of multiple key miRNAs that play a role in this process. Furthermore, altered *Hand2/Tbx3/Gli3* expression may be one of many regulatory changes that ultimately lead to the limb shift phenotype. In the context of these considerations, our model is consistent with existing data from us and others, and provides a plausible mechanism that miRNA inhibition of HAND2/TBX3 expression contributes to the

essential role of *Dicer* in positioning the limb bud. The conclusion that collectively, miRNAs are not essential for driving limb bud initiation, but rather for regulating limb bud positioning, is in accordance with the emerging theme that miRNAs act to fine tune development and homeostasis (Gantier et al., 2007; Schratt, 2009; Wienholds et al., 2003).

Materials and Methods

Generation of *Tcre;Dicer* mutants

Female mice homozygous for a *Dicer* conditional allele (*Dicer^flox^*) were mated to *Tcre* transgenic males carrying one *Dicer^flox^* or one *Dicer* deletion allele (*Dicer^del^*) allele to generate *Tcre;Dicer^flox/flox^* or *Tcre;Dicer^del/flox^* mutant embryos. No difference in phenotype is observed in mutant embryos of these two genotypes. The yolk sac or the brain of the embryos were taken for genotyping using the following PCR primer pairs: for Cre, 5′-TGATGAGGTTCGCAAGAACC-3′ and 5′-CCATGAGTGAACGAACCTGG-3′ (product size: 420bps); for *Dicer*, 5′-CCTGACAGTGACGGTCCAAAG-3′ and 5′-CATGACTCTTCAACTCAAACT-3′ (product sizes: 420 bps from the *Dicer^flox^* allele and 351 bps from the wild-type *Dicer* allele).

Embryo isolation and phenotype analyses

Embryos were dissected from time-mated mice, counting noon on the day the vaginal plug was found as embryonic day (E) 0.5. Whole mount in situ hybridization was performed as previously described (Neubuser et al., 1997).

For whole mount cell death detection, freshly dissected embryos were stained using LysoTracker Red DND-99 (Molecular Probes) as previously described (Zucker et al., 1999). Immunofluorescence staining was performed as previously described (Sun et al., 2002). The following antibodies were used: anti-MYF5 (Santa Cruz Biotechnology sc-302), anti-PAX7 (The Developmental Studies Hybridoma Bank), anti-CASPASE3 (Cell Signaling #9661). TUNEL staining was performed according to the manufacture's protocol (Roche).

Small RNA Northern blot analysis

RNA was isolated from E10.5 hindlimb bud and tail region with TRI® Reagent (Sigma). Approximately 20 μg of total RNA was loaded per lane on 10% urea/polyacrylamide gels and transferred to Hybond N$^+$ membranes (Amersham). Blots were prehybridized for 1 hour at 37°C before overnight incubation at 37°C in hybridization buffer containing [^{32}P]-end-labeled probe. Probes were generated by end-labeling 20 pmols of DNA oligonucleotide (Invitrogen) complementary to miRNA or U6 with T4 polynucleotide kinase (New England Biolabs) and 250 μCi [g-^{32}P] ATP (Perkin Elmer) followed by purification with MicroSpin™ G-25 columns (Amersham). Blots were washed (2X SSC, 0.1% SDS) at 37°C for 30 minutes followed by two 30 minutes room temperature washes and exposed to Kodak BioMax film.

Quantitative RT-PCR (qRT-PCR) analysis

E9.5 forelimb bud region, E10 hindlimb field (LPM between somite 25–28 region) and interlimb LPM were dissected from *Tcre;Dicer* mutants and control littermates. Total RNA was prepared using TRIzol (Invitrogen). For qRT-PCR of mRNA, first-strand synthesis was carried out using the Superscript III First Strand cDNA Synthesis Kit (Invitrogen). Quantitative PCR was performed using SYBR Green PCR Master Mix (Applied Biosystems) and the following primer pairs: for *Hand2*, 5′-TTCAAGGCGGAGATCAAGAAGACC-3′ and 5′-TCTTGTCGTTGCTGCTCACTGTGC-3′; for *Tbx3*, 5′-TCAACTGCTTTGCCCAGGCATCCTC-3′ and 5′-

CTTCGCTGGGACACAGATCTTTGA-3′; for *Gli3*, 5′-GTGCCTCCAGGTGAAGACTGTCAAG-3′ and 5′-GGGACTGTTGGCTGCTGCATGAAGA-3′; for *β-actin*, 5′-TGGGTCAGAAGGACTCCTATGTG-3′ and 5′-GTGGTACGACCAGAGGCATACAG-3′. Expression values were normalized using *β-actin*. For *mir-363* qRT-PCR, reverse transcription was performed using TaqMan MicroRNA Reverse Transcription Kit (Applied Biosystems) and primers specific to *mir-363* and *snoRNA202* (Applied Biosystems). qPCR was performed using TaqMan Universal Master Mix II (Applied Biosystems). Expression values of *mir-363* were normalized to *snoRNA202*. The results were compared using Student's *t*-test and reported as mean±S.D., and differences were considered statistically significant if p-value 0.05. Similar statistical methods were used for luciferase assays described below.

3′UTR Luciferase assay

The 3′ UTR of *Tbx3* and *Hand2* were amplified using the following primers: for *Tbx3*, 5′-GTTGCTTTGAAACGCGGGACTGAG-3′ and 5′-GGTCTAGAAAGTGGAGCCCGGAAGGGCCATTAC-3′; for *Hand2*, 5′-CGGGCTCTAGAAGAAGAGGAGAGCAGTGAGCCG-3′ and 5′-CGGGCTCTAGAGATAATTTAGTTTACTTCTGAATATTTT-3′. The PCR product was inserted into *pGl3c* vector (Promega) at XbaI site downstream of luciferase open reading frame. The *mir-363* sites were mutated by PCR mutagenesis. The following primers were used to mutate the sites: for *Tbx3*, 5′-AAAACCTTGTTCGGTCATATACAGTTAAAAGAACTAATGG-3′ and 5′-CTGTATATGACCGAACAAGGTTTTAAAAGATAATA-3′; for *Hand2*, 5′-GCCACACATAAATAAACCGGATGATCCA-3′ and 5′-GTTTATTTATGTGTGGCTTCCTTCCCCTTCT-3′.

In 24-well plates, Hela cells were grown to 90% confluence. Cells in each well were transfected with 120ng of *pGl3c*, 30ng of *TK-hRL* (Promega) as internal control, and 20pmol *pre-miR-363* or negative control #2 (Ambion) using 1ul lipofectamine 2000 (Invitrogen). Cells were lysed 48 hours later and assayed by using the Dual Luciferase kit (Promega).

Supplementary Material

Refer to Web version on PubMed Central for supplementary material.

Acknowledgments

References

Agarwal P, Wylie JN, Galceran J, Arkhitko O, Li C, Deng C, Grosschedl R, Bruneau BG. Tbx5 is essential for forelimb bud initiation following patterning of the limb field in the mouse embryo. Development. 2003; 130:623–633. [PubMed: 12490567]

Baek D, Villen J, Shin C, Camargo FD, Gygi SP, Bartel DP. The impact of microRNAs on protein output. Nature. 2008; 455:64–71. [PubMed: 18668037]

Bartel DP. MicroRNAs: target recognition and regulatory functions. Cell. 2009; 136:215–233. [PubMed: 19167326]

Bernstein E, Kim SY, Carmell MA, Murchison EP, Alcorn H, Li MZ, Mills AA, Elledge SJ, Anderson KV, Hannon GJ. Dicer is essential for mouse development. Nat Genet. 2003; 35:215–217. [PubMed: 14528307]

Bessho Y, Sakata R, Komatsu S, Shiota K, Yamada S, Kageyama R. Dynamic expression and essential functions of Hes7 in somite segmentation. Genes Dev. 2001; 15:2642–2647. [PubMed: 11641270]

Boulet AM, Moon AM, Arenkiel BR, Capecchi MR. The roles of Fgf4 and Fgf8 in limb bud initiation and outgrowth. Dev Biol. 2004; 273:361–372. [PubMed: 15328019]

Cohn MJ, Patel K, Krumlauf R, Wilkinson DG, Clarke JD, Tickle C. Hox9 genes and vertebrate limb specification. Nature. 1997; 387:97–101. [PubMed: 9139829]

Darnell DK, Kaur S, Stanislaw S, Konieczka JK, Yatskievych TA, Antin PB. MicroRNA expression during chick embryo development. Dev Dyn. 2006; 235:3156–3165. [PubMed: 17013880]

Dequeant ML, Pourquie O. Segmental patterning of the vertebrate embryonic axis. Nat Rev Genet. 2008; 9:370–382. [PubMed: 18414404]

Diez del Corral R, Olivera-Martinez I, Goriely A, Gale E, Maden M, Storey K. Opposing FGF and retinoid pathways control ventral neural pattern, neuronal differentiation, and segmentation during body axis extension. Neuron. 2003; 40:65–79. [PubMed: 14527434]

Fernandez-Teran M, Piedra ME, Simandl BK, Fallon JF, Ros MA. Limb initiation and development is normal in the absence of the mesonephros. Dev Biol. 1997; 189:246–255. [PubMed: 9299117]

Fukagawa T, Nogami M, Yoshikawa M, Ikeno M, Okazaki T, Takami Y, Nakayama T, Oshimura M. Dicer is essential for formation of the heterochromatin structure in vertebrate cells. Nat Cell Biol. 2004; 6:784–791. [PubMed: 15247924]

Gantier MP, Sadler AJ, Williams BR. Fine-tuning of the innate immune response by microRNAs. Immunol Cell Biol. 2007; 85:458–462. [PubMed: 17621315]

Gibert Y, Gajewski A, Meyer A, Begemann G. Induction and prepatterning of the zebrafish pectoral fin bud requires axial retinoic acid signaling. Development. 2006; 133:2649–2659. [PubMed: 16774994]

Giraldez AJ, Cinalli RM, Glasner ME, Enright AJ, Thomson JM, Baskerville S, Hammond SM, Bartel DP, Schier AF. MicroRNAs regulate brain morphogenesis in zebrafish. Science. 2005; 308:833–838. [PubMed: 15774722]

Gros J, Manceau M, Thome V, Marcelle C. A common somitic origin for embryonic muscle progenitors and satellite cells. Nature. 2005; 435:954–958. [PubMed: 15843802]

Harfe BD, McManus MT, Mansfield JH, Hornstein E, Tabin CJ. The RNaseIII enzyme Dicer is required for morphogenesis but not patterning of the vertebrate limb. Proc Natl Acad Sci U S A. 2005; 102:10898–10903. [PubMed: 16040801]

Harris KS, Zhang Z, McManus MT, Harfe BD, Sun X. Dicer function is essential for lung epithelium morphogenesis. Proc Natl Acad Sci U S A. 2006

Huang R, Zhi Q, Patel K, Wilting J, Christ B. Contribution of single somites to the skeleton and muscles of the occipital and cervical regions in avian embryos. Anatomy and embryology. 2000; 202:375–383. [PubMed: 11089929]

Jouve C, Palmeirim I, Henrique D, Beckers J, Gossler A, Ish-Horowicz D, Pourquie O. Notch signalling is required for cyclic expression of the hairy-like gene HES1 in the presomitic mesoderm. Development. 2000; 127:1421–1429. [PubMed: 10704388]

Kloosterman WP, Wienholds E, de Bruijn E, Kauppinen S, Plasterk RH. In situ detection of miRNAs in animal embryos using LNA-modified oligonucleotide probes. Nat Methods. 2006; 3:27–29. [PubMed: 16369549]

Krek A, Grun D, Poy MN, Wolf R, Rosenberg L, Epstein EJ, MacMenamin P, da Piedade I, Gunsalus KC, Stoffel M, Rajewsky N. Combinatorial microRNA target predictions. Nat Genet. 2005; 37:495–500. [PubMed: 15806104]

Naiche LA, Mark Lewandoski NH. FGF4 and FGF8 comprise the wavefront activity that controls somitogenesis. Proc Natl Acad Sci U S A. 2010

Lai EC, Tam B, Rubin GM. Pervasive regulation of Drosophila Notch target genes by GY-box-, Brd-box-, and K-box-class microRNAs. Genes Dev. 2005; 19:1067–1080. [PubMed: 15833912]

Lee RC, Feinbaum RL, Ambros V. The C. elegans heterochronic gene lin-4 encodes small RNAs with antisense complementarity to lin-14. Cell. 1993; 75:843–854. [PubMed: 8252621]

Lewis BP, Burge CB, Bartel DP. Conserved seed pairing, often flanked by adenosines, indicates that thousands of human genes are microRNA targets. Cell. 2005; 120:15–20. [PubMed: 15652477]

Lewis BP, Shih IH, Jones-Rhoades MW, Bartel DP, Burge CB. Prediction of mammalian microRNA targets. Cell. 2003; 115:787–798. [PubMed: 14697198]

Martin GR. The roles of FGFs in the early development of vertebrate limbs. Genes Dev. 1998; 12:1571–1586. [PubMed: 9620845]

McIntyre DC, Rakshit S, Yallowitz AR, Loken L, Jeannotte L, Capecchi MR, Wellik DM. Hox patterning of the vertebrate rib cage. Development (Cambridge, England). 2007; 134:2981–2989.

McPherron AC, Lawler AM, Lee SJ. Regulation of anterior/posterior patterning of the axial skeleton by growth/differentiation factor 11. Nat Genet. 1999; 22:260–264. [PubMed: 10391213]

Minguillon C, Del Buono J, Logan MP. Tbx5 and Tbx4 are not sufficient to determine limb-specific morphologies but have common roles in initiating limb outgrowth. Dev Cell. 2005; 8:75–84. [PubMed: 15621531]

Moreno TA, Kintner C. Regulation of segmental patterning by retinoic acid signaling during Xenopus somitogenesis. Dev Cell. 2004; 6:205–218. [PubMed: 14960275]

Morimoto M, Sasaki N, Oginuma M, Kiso M, Igarashi K, Aizaki K, Kanno J, Saga Y. The negative regulation of Mesp2 by mouse Ripply2 is required to establish the rostro-caudal patterning within a somite. Development. 2007; 134:1561–1569. [PubMed: 17360776]

Naiche LA, Papaioannou VE. Loss of Tbx4 blocks hindlimb development and affects vascularization and fusion of the allantois. Development. 2003; 130:2681–2693. [PubMed: 12736212]

Neubuser A, Peters H, Balling R, Martin GR. Antagonistic interactions between FGF and BMP signaling pathways: a mechanism for positioning the sites of tooth formation. Cell. 1997; 90:247–255. [PubMed: 9244299]

Nomura-Kitabayashi A, Takahashi Y, Kitajima S, Inoue T, Takeda H, Saga Y. Hypomorphic Mesp allele distinguishes establishment of rostrocaudal polarity and segment border formation in somitogenesis. Development. 2002; 129:2473–2481. [PubMed: 11973278]

O'Rourke JR, Georges SA, Seay HR, Tapscott SJ, McManus MT, Goldhamer DJ, Swanson MS, Harfe BD. Essential role for Dicer during skeletal muscle development. Dev Biol. 2007; 311:359–368. [PubMed: 17936265]

Palmeirim I, Henrique D, Ish-Horowicz D, Pourquie O. Avian hairy gene expression identifies a molecular clock linked to vertebrate segmentation and somitogenesis. Cell. 1997; 91:639–648. [PubMed: 9393857]

Perantoni AO, Timofeeva O, Naillat F, Richman C, Pajni-Underwood S, Wilson C, Vainio S, Dove LF, Lewandoski M. Inactivation of FGF8 in early mesoderm reveals an essential role in kidney development. Development. 2005; 132:3859–3871. [PubMed: 16049111]

Rallis C, Del Buono J, Logan MP. Tbx3 can alter limb position along the rostrocaudal axis of the developing embryo. Development. 2005; 132:1961–1970. [PubMed: 15790970]

Relaix F, Rocancourt D, Mansouri A, Buckingham M. A Pax3/Pax7-dependent population of skeletal muscle progenitor cells. Nature. 2005; 435:948–953. [PubMed: 15843801]

Saga Y. Segmental border is defined by the key transcription factor Mesp2, by means of the suppression of Notch activity. Dev Dyn. 2007; 236:1450–1455. [PubMed: 17394251]

Saga Y, Hata N, Koseki H, Taketo MM. Mesp2: a novel mouse gene expressed in the presegmented mesoderm and essential for segmentation initiation. Genes Dev. 1997; 11:1827–1839. [PubMed: 9242490]

Schratt G. Fine-tuning neural gene expression with microRNAs. Curr Opin Neurobiol. 2009; 19:213–219. [PubMed: 19539460]

Selbach M, Schwanhausser B, Thierfelder N, Fang Z, Khanin R, Rajewsky N. Widespread changes in protein synthesis induced by microRNAs. Nature. 2008; 455:58–63. [PubMed: 18668040]

Stefani G, Slack FJ. Small non-coding RNAs in animal development. Nat Rev Mol Cell Biol. 2008; 9:219–230. [PubMed: 18270516]

Sun X, Mariani FV, Martin GR. Functions of FGF signalling from the apical ectodermal ridge in limb development. Nature. 2002; 418:501–508. [PubMed: 12152071]

te Welscher P, Fernandez-Teran M, Ros MA, Zeller R. Mutual genetic antagonism involving GLI3 and dHAND prepatterns the vertebrate limb bud mesenchyme prior to SHH signaling. Genes Dev. 2002; 16:421–426. [PubMed: 11850405]

van den Akker E, Fromental-Ramain C, de Graaff W, Le Mouellic H, Brulet P, Chambon P, Deschamps J. Axial skeletal patterning in mice lacking all paralogous group 8 Hox genes. Development (Cambridge, England). 2001; 128:1911–1921.

Wienholds E, Kloosterman WP, Miska E, Alvarez-Saavedra E, Berezikov E, de Bruijn E, Horvitz RH, Kauppinen S, Plasterk RH. MicroRNA Expression in Zebrafish Embryonic Development. Science. 2005

Wienholds E, Koudijs MJ, van Eeden FJ, Cuppen E, Plasterk RH. The microRNA-producing enzyme Dicer1 is essential for zebrafish development. Nat Genet. 2003; 35:217–218. [PubMed: 14528306]

Wightman B, Ha I, Ruvkun G. Posttranscriptional regulation of the heterochronic gene lin-14 by lin-4 mediates temporal pattern formation in C. elegans. Cell. 1993; 75:855–862. [PubMed: 8252622]

Yang WJ, Yang DD, Na S, Sandusky GE, Zhang Q, Zhao G. Dicer is required for embryonic angiogenesis during mouse development. J Biol Chem. 2005; 280:9330–9335. [PubMed: 15613470]

Zhao Y, Samal E, Srivastava D. Serum response factor regulates a muscle-specific microRNA that targets Hand2 during cardiogenesis. Nature. 2005; 436:214–220. [PubMed: 15951802]

Zucker RM, Hunter ES 3rd, Rogers JM. Apoptosis and morphology in mouse embryos by confocal laser scanning microscopy. Methods (San Diego, Calif. 1999; 18:473–480.

Research highlights

Dicer is essential for paraxial mesodermal cell survival;

Dicer is essential for establishing rostral-caudal polarity of somites;

Paraxial mesoderm segmentation occurs in the absence of Dicer;

Dicer is essential for hindlimb bud positioning;
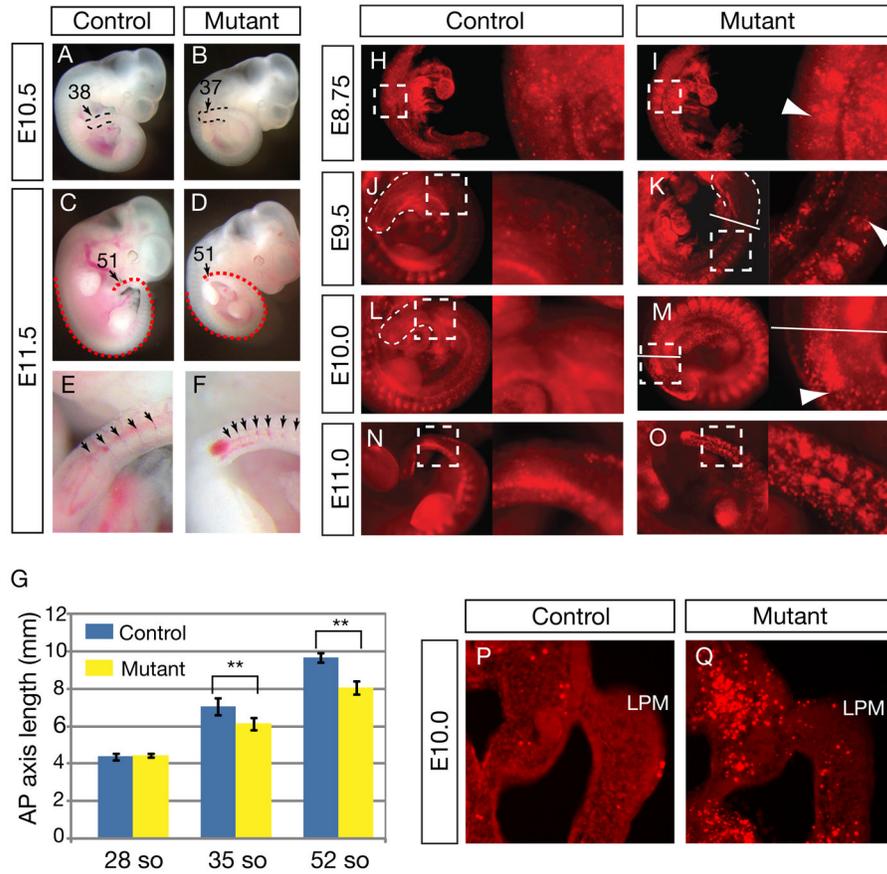
Dicer may act via miRNAs to control Hand2/Tbx3 expression and limb positioning.

Figure 1. *Tcre;Dicer* mutants display a shorter axis due to increased cell death
(A–F) Gross morphology of *Tcre;Dicer* mutant embryos. Here, as in all figures, each littermate pair of control and mutant embryos are shown at the same magnification. Dashed lines in A,B outline the tails. Dash lines in C and D exemplify the paths for A-P axis measurements shown in G. Arrows in A-D indicate the most posterior somites and their numbers. E and F are enlarged views of the tails shown in C and D. Arrows illustrate that clear boundaries form in the mutant, and mutant somites are smaller compared to control (see also sections in Supplemental Fig. 2). (G) Length of AP-axis starting from posterior boundary of forelimb and ending at tail tip (n 4 for either control or mutant embryos at each stage, **: p 0.01; 28-somite stage: control 4.38±0.16mm, mutant:4.43±0.10mm, p=0.29; 35-somite stage: control 7.07±0.47mm, mutant 6.14±0.33mm, p=0.0033; 52-somite stage: control 9.67±0.26mm, mutant 8.08±0.36mm, p=0.0003). (H–O) Control and mutant embryos were stained with LysoTracker to label apoptotic cells with red punctate signals. Equivalent regions are boxed in controls and mutants, and are enlarged on the right. White lines in K and M mark the anterior boundary of PSM, and arrowheads in I, K and M mark the posterior boundary of increased cell death. Dashed lines in J-L outline the tail. (H,I) At E8.75 (~15 somite stage), increased cell death is observed in the mutant embryo in somites 5 and 6. (J,K) At E9.5 (~24 somite stage), increased cell death is detected in the mutant embryo in all somites at and posterior to somite 5, with the exception of the nascent 2–3 somites and PSM. (L,M) At E10 (~30 somite stage), the posterior boundary of increased cell death in the mutant embryo extends into anterior PSM. (N,O) At E11 (~40 somite stage), increased cell death has extended into the entire PSM in the mutant. (P,Q) Transverse section of Lysotracker-stained E10 embryos in the interlimb region.
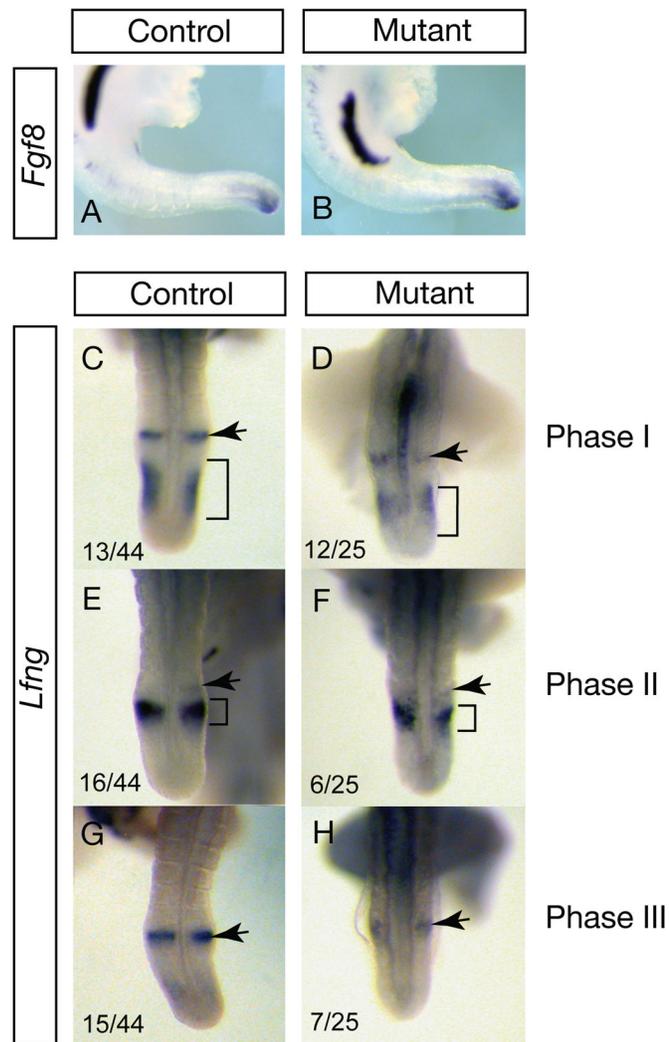
Figure 2. The molecular machinery for PSM segmental patterning remains normal in *Tcre;Dicer* embryos

Clock and wave front markers are assayed by RNA in situ hybridization in E10.5 embryos. (A, B) *Fgf8* expression remains normal in the mutant compared to control. (C–H) All three phases of *Lfng* oscillation (bracketed in each phase) were observed in the mutant PSM. The number of embryos observed in each phase in proportion to the total number of embryos assayed for either control (n=44) or mutant (n=25) is shown at the left-bottom corner of each panel. For all phases, the weaker expression in the mutant is likely a result of increased cell death. The strong axial signal shown in D and H are due to non-specific probe trapping in the neural tube.
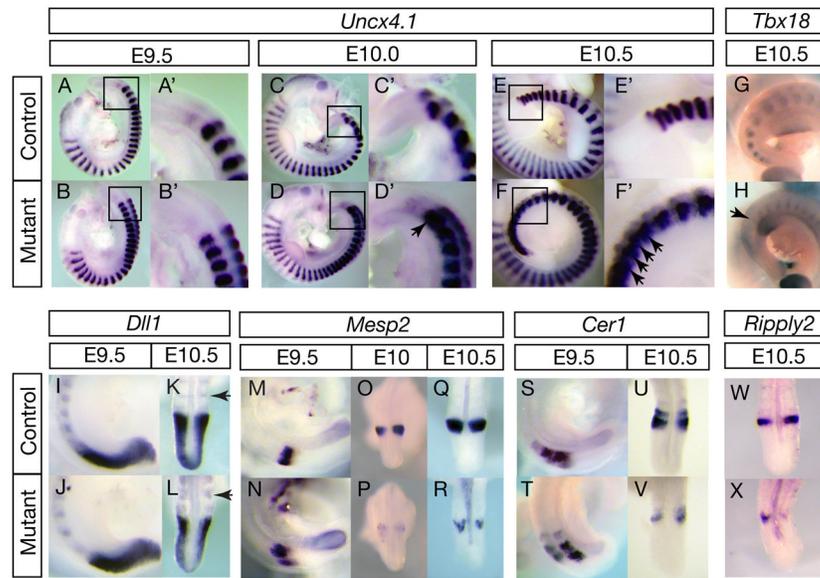
Figure 3. Loss of rostral-caudal polarity in *Tcre;Dicer* somites
Rostral-caudal markers as assayed by RNA in situ hybridization. (A -F′) The expression of
Uncx4.1, a caudal somite marker, is expanded in the nascent somites in the mutant starting
at E10.0. A′– F′ are magnified views of the boxed areas in A-F, respectively. Arrows in D′
and F′ indicate caudalized somites. (G,H) Expression of *Tbx18*, a rostral somite marker, is
reduced in the mutant as indicated by arrow in H. (I–L) Expression of *Dll1*, a caudal marker
in nascent somites, is normal at E9.5, but expanded by E10.5 in the mutant compared to
control (arrows). (M–R) Expression of *Mesp2* is normal at E9.5, but is downregulated
starting at E10. (S–V) Expression of *Cer1*, a downstream target of *Mesp2*, is normal at E9.5,
but is downregulated by E10.5. (W,X) Expression of *Ripply2*, a repressor of *Mesp2*, is
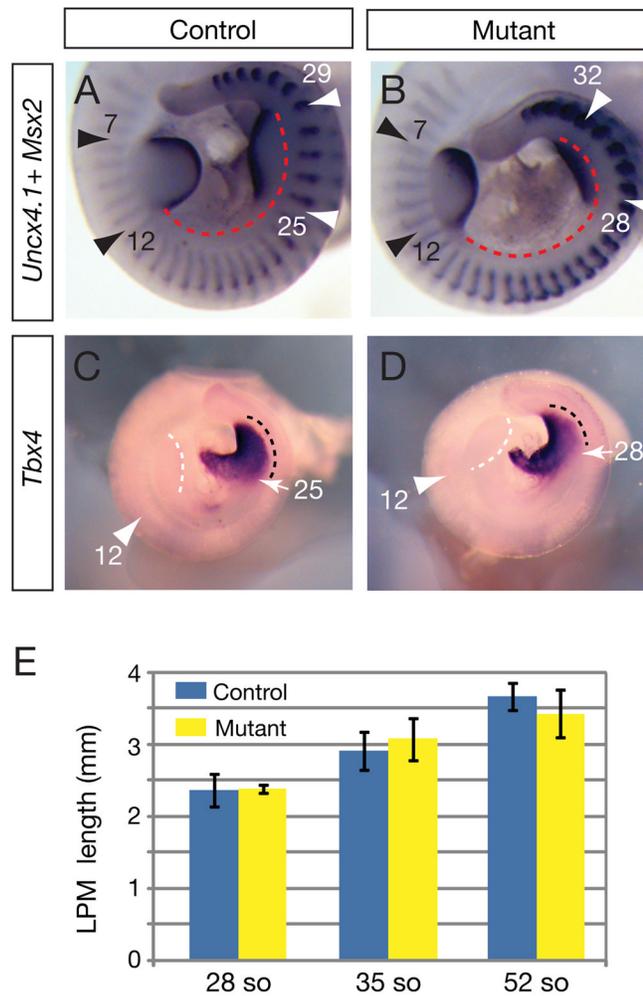downregulated at E10.5.

Figure 4. Posterior shift of hindlimb buds in *Tcre;Dicer* mutant
Limb bud position as outlined by RNA in situ. (A–B) Expression of somite marker *Uncx4.1*
and limb bud marker *Msx2* at E10.5. The black and white arrowheads indicate the anterior
and posterior boundaries (indicated in somite numbers) of the forelimb and hindlimb buds,
respectively. Dash lines in A and B exemplify the paths for LPM measurements shown in E.
(C,D) Expression of hindlimb bud marker *Tbx4* at E10.0. The white dash lines outline the
forelimb buds. Arrowheads indicate the posterior boundary of the forelimb buds and
corresponding somite number. Arrows indicate the anterior boundaries of hindlimb buds and
corresponding somite number. Black dash lines outline the extent of *Tbx4* expression in the
prospective limb LPM. (E) Length of LPM starting from posterior boundary of forelimb and
ending at posterior boundary of hindlimb (n 4 control and mutant embryos at each stage;
28-somite stage: control 2.36±0.23mm, mutant 2.39±0.06mm, p=0.41; 35-somite stage:
control 2.91±0.27mm, mutant 3.08±0.29mm, p=0.18; 52-somite stage: control 3.66
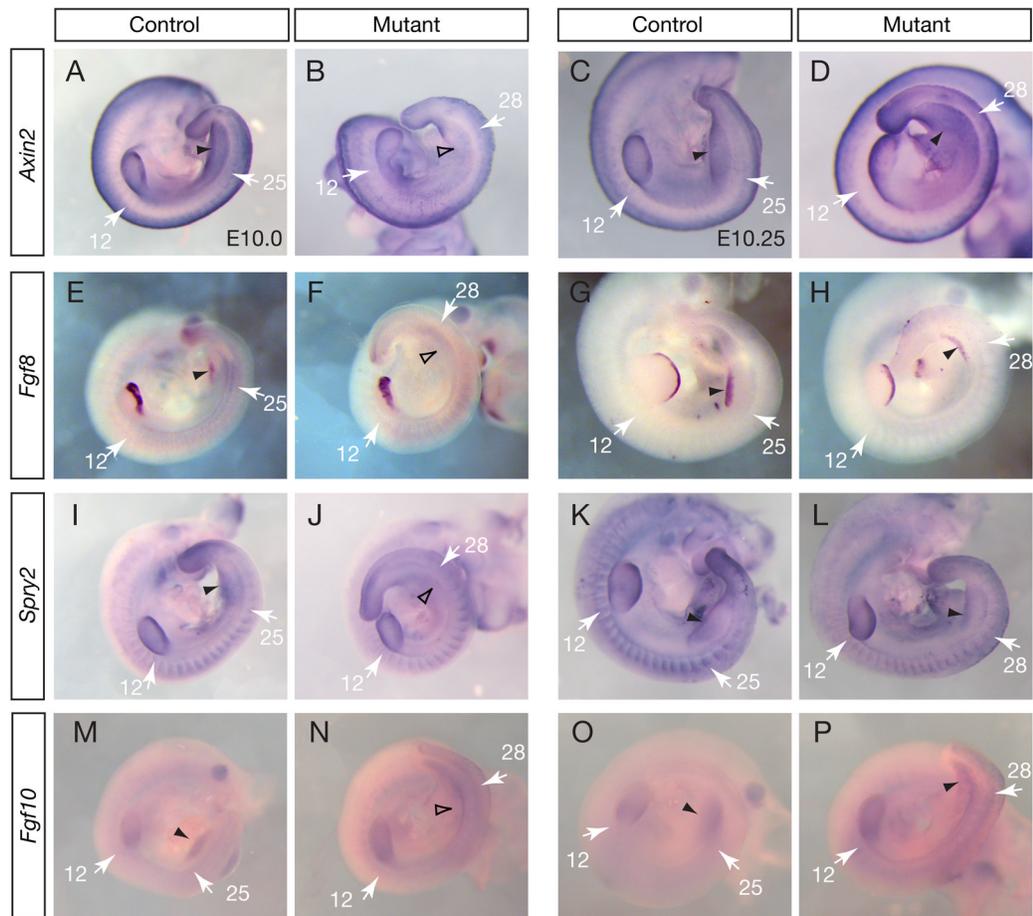±0.19mm, mutant 3.43±0.33mm, p=0.13).

Figure 5. Expression of FGF and WNT pathway genes is delayed and posteriorly shifted in *Tcre;Dicer* mutant
Gene expression as assayed by RNA situ hybridization at E10 (left) or E10.25 (right). Arrows indicate the posterior boundary of forelimb or anterior boundary of hindlimb. Filled arrowheads indicate presence of expression in the hindlimb bud field. Open arrowheads indicate lack of expression in the mutant LPM at the A-P position corresponding to the nascent hindlimb bud in the control.
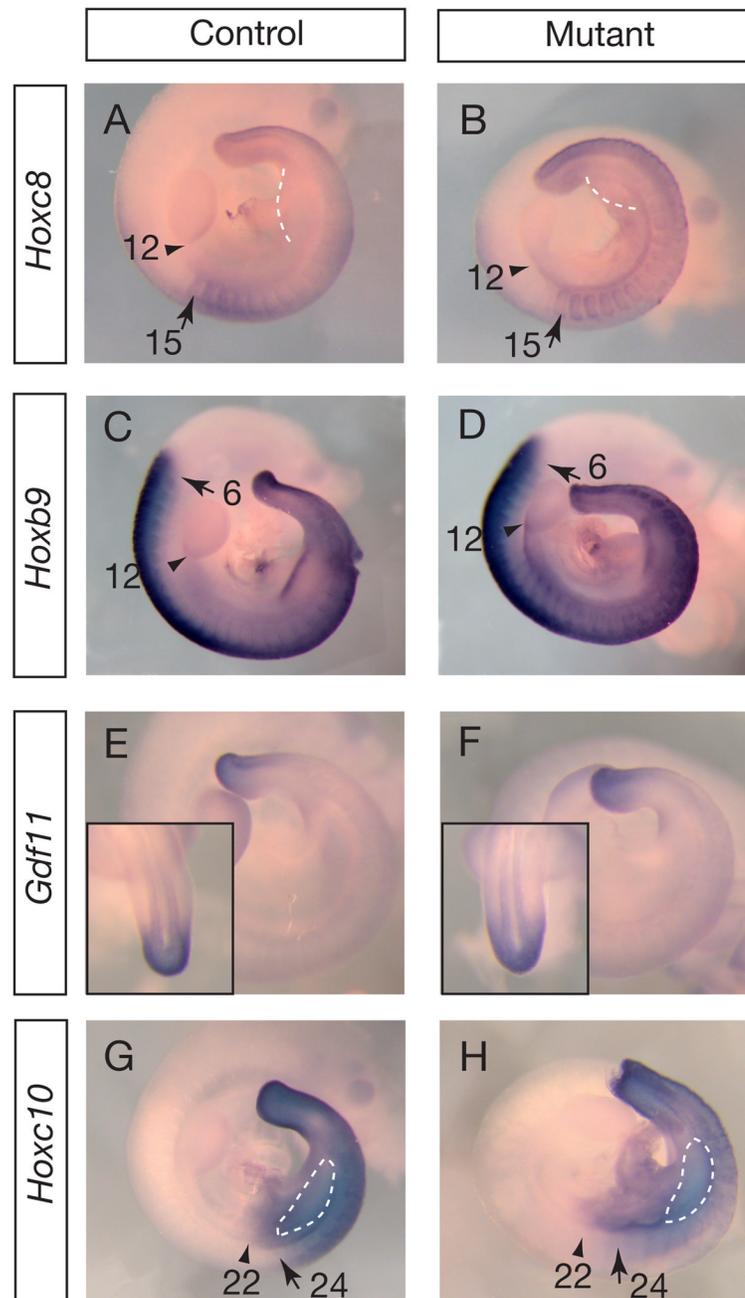
Figure 6. Expression of Hox genes and *Gdf11* remains normal in *Tcre;Dicer* mutant, despite of hindlimb bud shift

Gene expression as assayed by RNA situ hybridization at E10.25. Arrows and arrowheads indicate the approximate anterior boundaries and somite numbers of the expression domain in paraxial mesoderm and LPM, respectively. Insets in E and F are dorsal view of tail bud region. Dashed lines in A,B,G,H indicate the position of hindlimb buds.
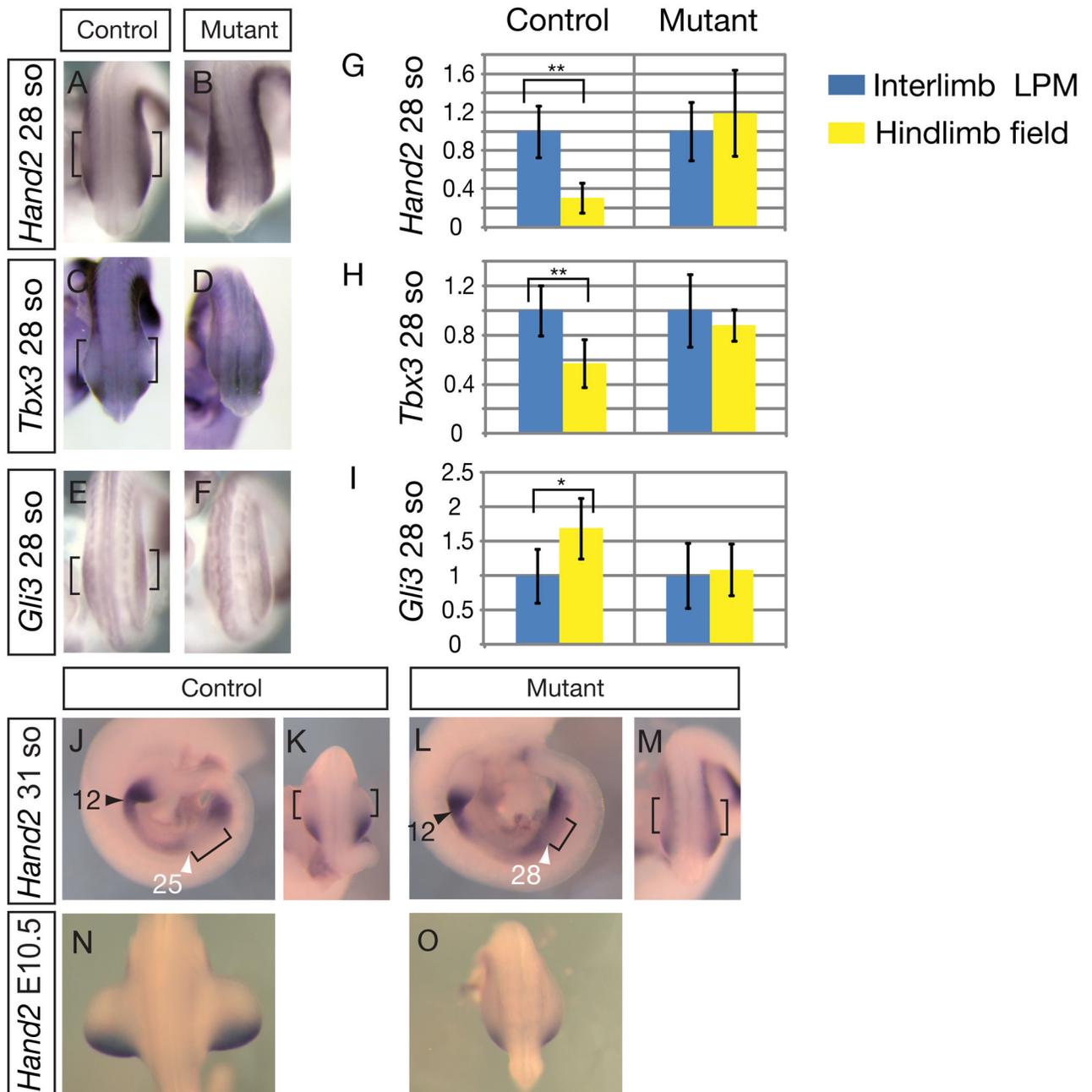
Figure 7. Expression of *Hand2* and *Tbx3* persists during hindlimb bud initiation in the *Tcre;Dicer* mutant

(A–F) Gene expression as assayed by RNA in situ hybridization during hindlimb bud initiation (~28-somite stage, dorsal views). In control embryos, brackets indicate the prospective anterior hindlimb bud region where expression of *Hand2* and *Tbx3* is downregulated, and expression of *Gli3* is upregulated. In mutant littermates at the equivalent region, *Hand2* and *Tbx3* are not downregulated, and *Gli3* is not upregulated. (G–I) qRT-PCR analysis of gene expression at ~28-somite stage. The expression levels in hindlimb field was compared to interlimb LPM. *Hand2* hindlimb vs LPM: control 0.31±0.16 (n=4, p=0.0006), mutant 1.19±0.44 (n=6, p=0.20); *Tbx3* hindlimb vs LPM control 0.57±0.20 (n=6, p=0.002), mutant 0.88±0.13 (n=4, p=0.24); *Gli3* hindlimb vs LPM: control 1.69±0.44

(n=5, p=0.015), mutant 1.09±0.37 (n=5, p=0.38)*: p 0.05. **:p 0.01. (J–O) *Hand2* expression as assayed by RNA in situ hybridization at 31-somite stage and E10.5. The black and white arrowheads indicate the posterior or anterior boundary (indicated in somite numbers) of the forelimb and hindlimb buds, respectively. Expression of *Hand2* is downregulated at these stages in a more posterior domain.
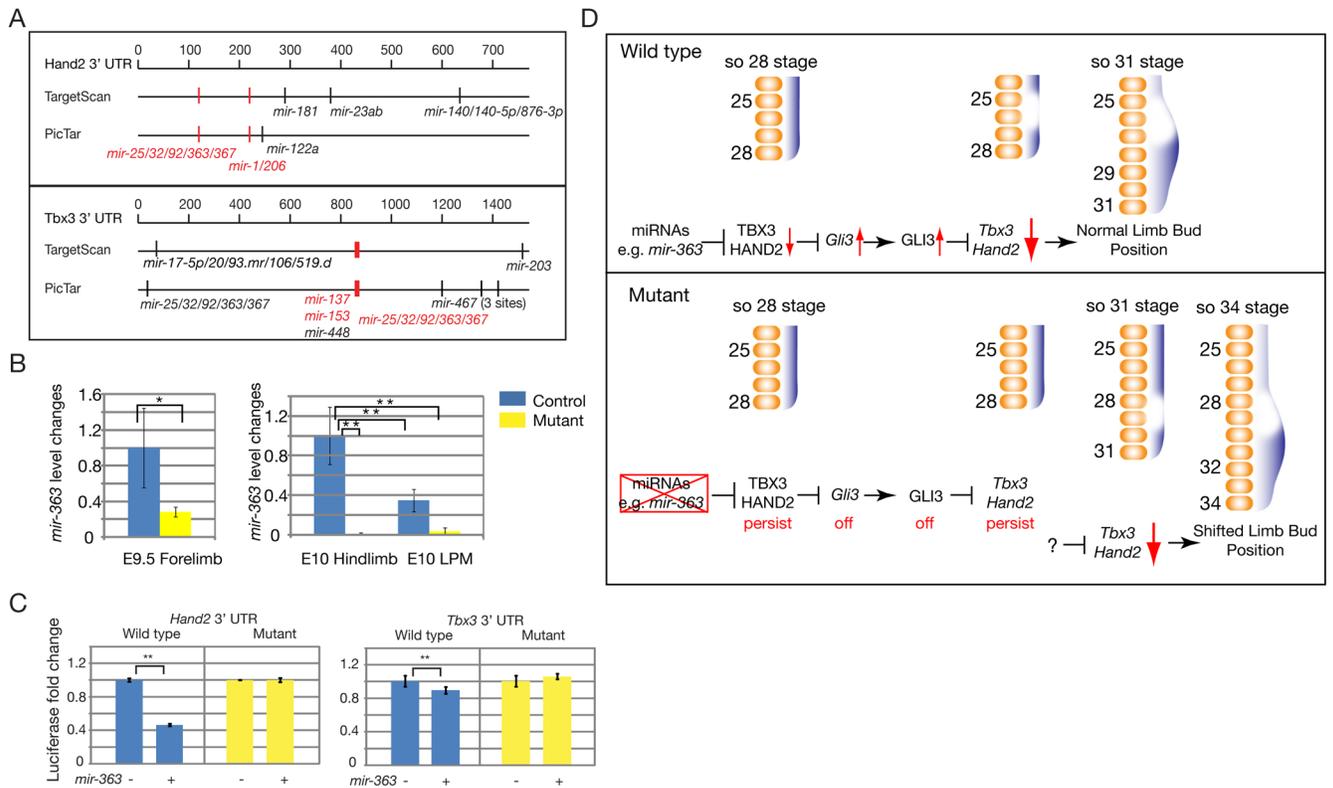
Figure 8. Expression of *Hand2* and *Tbx3* is regulated by *mir-363* in vitro
(A) Predicted miRNA target sites in the 3′ UTR of *Hand2* and *Tbx3* by TargetScan and
PicTar. The sites predicted by both programs are marked in red. (B) qRT-PCR analysis of
mir-363 expression in forelimb region at E9.5 and hindlimb and interlimb LPM at E10.
E9.5: mutant vs control 0.28±0.06 (n=3, p=0.026); E10: mutant hindlimb vs control
hindlimb 0.010±0.01(n=3, p=0.002), control LPM vs control hindlimb 0.35±0.11 (n=3,
p=0.01), mutant LPM vs control hindlimb 0.037±0.033 (n=3, p=0.002). *:p 0.05, **
p 0.01. (C) Luciferase assay to test the effect of *mir-363* on *Hand2* and *Tbx3* expression via
their 3′ UTRs. Wild-type or a mutant (with *mir-363* site mutated) *Hand2* or *Tbx3* 3′UTR
were inserted downstream of luciferase. The constructs were co-transfected with either pre-
miRNA scrambled control or pre-*mir-363* into Hela cells. *mir-363* represses the luciferase
activity via wild-type *Hand2* 3′UTR to 46±1.5% (n=3, p=1.5E-6), and via wild-type *Tbx3*
3′UTR to 89±4.1% (n=6, p=0.004). In each case, the repression is lost when the predicted
target site is mutated (101±2%, n=3, p=0.38 for *Hand2* and 105±4%, n=6, p=0.07 for *Tbx3*).
**: p 0.01. (D) A model depicting a possible mechanism for miRNA control of hindlimb
bud positioning. Blue regions represent *Hand2* and *Tbx3* expression domains in the LPM,
adjacent to somites. In wild type embryos at the prospective anterior hindlimb bud level
(somite 25–28), miRNAs, for example *mir-363*, downregulate the expression of HAND2
and TBX3 proteins, which allows the expression of *Gli3* RNA. In turn, GLI3 protein
reinforces the downregulation of *Tbx3* and *Hand2* by inhibiting their expression at the
transcript level. The feedback among these genes establishes the position of the hindlimb
bud. In *Tcre;Dicer* mutant, downregulation of HAND2 and TBX3 transcript and protein
expression is delayed due to lack of mature miRNAs, preventing limb bud initiation at the
normal position. Approximately six hours later, a backup mechanism inhibits *Hand2/Tbx3*
in the LPM at a more posterior position, allowing limb bud initiation.